Quantum-Defect Electronegativity Scale for Nontransition Elements

Judith St. John* and Aaron N. Bloch†

Department of Chemistry, The Johns Hopkins University, Baltimore, Maryland 21218

(Received 22 July 1974)

We suggest that the Pauli-force model potential defines a new electronegativity scale consisting of explicit orbital components. These are determined algebraically from atomic spectral data. We find that these components distinguish quantitatively the most stable crystal structures of 34 nontransition elemental solids and 59 A^NB^{8-N} binary compounds.

Recently, Simons[1-4] and Simons and Bloch[5,6] have observed that much of the chemical content of an atomic pseudopotential can be expressed by a set of dimensionless parameters derived directly from atomic spectral data through simple algebraic relations. In this note we suggest that these parameters also define a scale of electronegativity for the nontransition elements. The new scale is in qualitative agreement with traditional ones, but is more refined in the sense that individual orbital contributions are explicitly defined. A discussion of hybridization in chemical bonding follows directly. Empirically we find that the average hybridization and total electronegativity form the basis for a series of two-dimensional plots which completely delineate the most stable crystal structures of the 34 elemental solids and 59 A^NB^{8-N} binary compounds for which appropriate spectral data are available. Among the elements we distinguish quantitatively the hcp, fcc, bcc, and covalent structures: among the binaries we separate zinc-blende, wurtzite, rock-salt, and cesium-chloride structures. Most of these distinctions are not made by more familiar scales of electronegativity and ionicity,[7-9] and some of them are normally accessible only to comparatively sophisticated calculations.[10]

Except in the immediate vicinity of the nucleus, the pseudopotential of a one-valence-electron ion is represented closely by the "Pauli-force" model potential introduced by Simons[1]:

$$V(r) = -\frac{Z}{r} + \sum_l \frac{\hat{l}(\hat{l}+1) - l(l+1)}{r^2} P_l \,, \tag{1}$$

with Z the net core charge, P_l the projection operator for orbital quantum number l, and $\hat{l}$ an l-dependent parameter. The potential (1) has a simple physical significance,[1,5] and has been successfully applied in studies of atoms,[1,2] molecules,[3,4,11] and solids.[5,6] A principal advantage is that it renders the one-electron radial Schrödinger equation exactly solvable. The eigenfunctions[1,5] are of hydrogenic form, with integral principal quantum number n but nonintegral orbital quantum number $\hat{l}$. The eigenvalues are

$$E(n, l) = -Z^2/2[n + \hat{l}(l) - l]^2 \,. \tag{2}$$

Clearly, all of the chemical information contained in the potential (1) resides in the core charge Z and the quantum defect $\hat{l}(l) - l$. The latter can be evaluated by fitting (2) to experiment[1,5,12]; a very simple scheme for doing so at energies appropriate to solids has been suggested elsewhere.[5,6]

Physically, the quantum defect is related through (2) to the depth of the potential well and the strength of the effective centrifugal barrier represented by (1). We shall find it particularly convenient to express these quantities in terms of the positions of the radial maxima of the unscreened, lowest valence eigenfunctions of (1):

$$r_l = \hat{l}(\hat{l}+1)/Z \,. \tag{3}$$

Now, Bloch and Simons[6] have suggested that among those elements for which only s and p bonding is important, the degree of s-p hybridization in the elemental solid is reflected in a "structural index,"

$$S \equiv (r_1 - r_0)/r_1 \,. \tag{4}$$

The index S is very nearly equal numerically to the fraction of "s character" estimated by Pauling[7] for the first-row elements, and its variation over the periodic table is closely correlated with trends in the crystal structures of the nontransition elements.[6]

This behavior was rationalized by Bloch and Simons[6] in terms of simple orbital geometries. While we consider such arguments to be qualitatively correct, it is clear that the radii r_l for ions of high Z are much too small to be compared directly with physically realistic bonding radii. We find it conceptually more satisfying, and more

consistent with chemical tradition, to redefine S in terms of an "orbital electronegativity,"

$$X_l \equiv 1/r_l , \tag{5}$$

whence

$$S = (X_0 - X_1)/X_0 . \tag{6}$$

"Electronegativity" has been variously defined,[13,14] but is by general consent some measure of the attractive interaction between a valence electron and the atomic core. The orbital components X_l, which measure the scattering power of the core for the lth partial wave, individually satisfy this criterion. They are related directly to the experimental quantum defect through (2), (3), and (5), and their differences reflect hybridizations through relations like (6). Their sum we take to determine the total electronegativity of the atom:

$$X \equiv a \sum_{l=0}^{2} X_l + b , \tag{7}$$

where we choose the constants $a = 0.43$ and $b = 0.24$ so as to reproduce the values arbitrarily assigned by Pauling to the first-row elements.

Unlike the traditional thermochemical scale of Pauling[7] and the dielectric scale of Phillips,[8] the electronegativity (7) is a purely atomic property, independent of molecular or crystalline environment. The three scales are compared in Table I. The new set of electronegativities falls between the other two, though somewhat closer to Pauling's values. It is interesting, however, that if the summation in (7) is truncated after $l = 1$, we obtain (after readjustment of a and b) excellent agreement with the scale of Phillips, which by definition contains only s-p contributions.

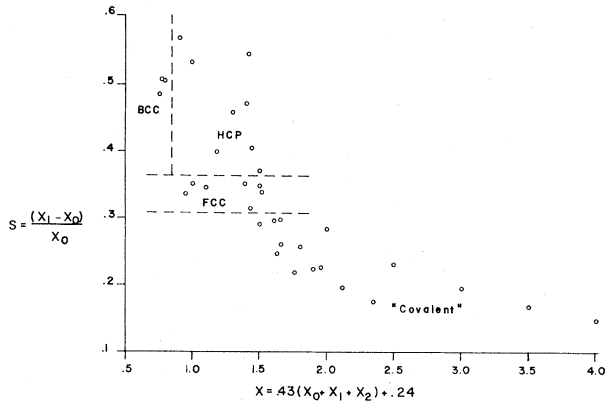

FIG. 1. Structural index versus electronegativity for the nontransition elements.

In Fig. 1 we plot S as a function of X for 34 nontransition elements. The plot cleanly separates these elements according to their most stable structures at zero temperature and pressure. The addition of the coordinate X represents a sophistication over the work of Bloch and Simons,[6] who were unable to account for the structures of the heavy alkali metals, for example, on the basis of the index S alone. In Fig. 1 these elements form the bcc section of the plot, with Li and Na just over the bcc-hcp border. (The last two undergo an hcp-bcc phase change as the temperature is raised from zero.[10]) Elsewhere, the plot exhibits the expected trends, with large "s characters" and small electronegativity favoring metallic strcutures. For simplicity, we have loosely classified as "covalent" all those elements whose band structures correspond to the formation of directional bonds,[10] whether or not there is band overlap to form a semimetal. Within this group, the metal-nonmetal trend is roughly monotonic in X and S: The elements closest to the fcc region are the semimetals Sn and Bi, followed by Sb, As, and Te, which also exhibit some metallic compounds. Over all, in the language of Ref. 6 the number of "bonding neighbors" (in the Pauling[7] sense) is largest when the core is diffuse, electropositive and s like, and smallest when it is compact, electronegative and p like.

Among the $A^N B^{8-N}$ binary compounds, we expect strong hybridization and small differences

TABLE I. Comparison of the quantum-defect electronegativity scale with those of Pauling, in parentheses, and Phillips, in brackets.

Li	Be		B	C	N	O	F
0.99	1.50		2.00	2.50	3.01	3.51	4.01
(1.0)	(1.5)		(2.0)	(2.5)	(3.0)	(3.5)	(4.0)
[1.00]	[1.50]		[2.00]	[2.50]	[3.00]	[3.50]	[4.00]
Na	Mg		Al	Si	P	S	Cl
0.91	1.18		1.43	1.66	1.90	2.12	2.35
(0.9)	(1.2)		(1.5)	(1.8)	(2.1)	(2.5)	(3.0)
[0.72]	[0.96]		[1.18]	[1.41]	[1.64]	[1.87]	[2.10]
K	Ca	Zn	Ga	Ge	As	Se	
0.79	1.10	1.40	1.50	1.66	1.81	1.96	
(0.8)	(1.0)	(1.6)	(1.6)	(1.8)	(2.0)	(2.4)	
[0.79]	[0.91]		[1.13]	[1.35]	[1.57]	[1.79]	
Rb	Sr	Cd	In	Sn	Sb	Te	
0.77	1.01	1.31	1.39	1.50	1.63	1.77	
(0.8)	(1.0)	(1.7)	(1.7)	(1.8)	(1.9)	(2.1)	
[0.66]	[0.83]		[0.99]	[1.15]	[1.31]	[1.47]	
Cs	Ba	Hg	Tl	Pb	Bi		
0.75	0.95	1.43	1.44	1.52	1.61		
(0.7)	(0.9)	(1.9)	(1.8)	(1.8)	(1.9)		
[0.64]	[0.79]		[0.94]	[1.09]	[1.24]		

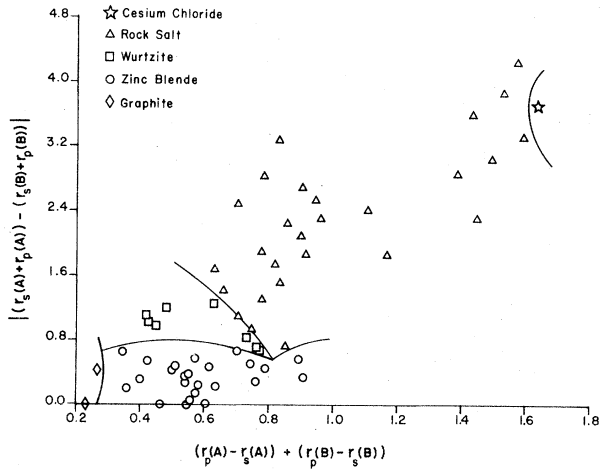

FIG. 2. Electronegativity difference versus average hybridization for the $A^N B^{8-N}$ binary compounds.

in electronegativity to favor covalent, tetrahedrally coordinated structures, and we find that a simple plot of electronegativity difference versus average hybridization does distinguish among fourfold, sixfold, and eightfold coordination. A much more detailed separation of structures, however, is afforded by Fig. 2, where we plot a nonnormalized measure of the s-p contribution to the electronegativity, $|[r_0(A)+r_1(A)] - [r_0(B)+r_1(B)]|$, against the corresponding nonnormalized s-p hybridization, $[r_1(A)-r_0(A)] + [r_1(B)-r_0(B)]$, for 59 binaries and four $Z=4$ elements. For dimorphous compounds, the structure indicated in the figure is the one most stable at zero temperature and pressure. Among the fourfold structures, the thermodynamic arguments of Jagodzinski[15] place in the zinc-blende category those materials (such as ZnS, ZnSe, ZnTe, CdTe, and SiC) which form polytypes,[16] and in the wurtzite section those (such as CdS and CdSe) which do not.[16] The wurtzite–rock-salt borderline we take to pass through or near MgS and MgSe, and the rock-salt–zinc-blende line near HgS. The eightfold CsCl structure stands alone at one extreme of the plot, and BN and C, which are most stable in the graphite structure, are isolated at the opposite end.

Figure 2 not only distinguishes among gross coordination numbers, but between the tetrahedrally coordinated zinc-blende and wurtzite structures as well. This is a third-neighbor effect, subtle enough to have eluded the plots of Mooser and Pearson,[17] and, in part, the dielectric ionicity scale of Phillips[9] (as expressed by the plots of Van Vechten[18]). Here the wurtzite structure is delineated in accord with simple electrostatic arguments and chemical intuition. The wurtzite structure, in which third neighbors of unlike charge are eclipsed, is more "ionic" than the zinc-blende structure, in which they are staggered.[16,19] For large electronegativity differences, then, wurtzite falls between zinc blende and rock salt in Fig. 2. As the ordinate, and with it the effective charge difference between A and B, diminishes, the eclipsed form is destabilized, and for very small electronegativity differences it does not occur at all. The trend is clearly reflected in the figure. Further, we find a 90% correlation between the ordinate of Fig. 2 and the c/a ratios of distorted wurtzite compounds.

We conclude that the quantum-defect electronegativity scale is a sensitive indicator of chemical trends in the structures of simple solids, and a potentially useful vehicle for relating them directly to their atomic antecedents. Extensions to more complex systems are in progress.

It is a pleasure to thank R. G. Parr, J. C. Phillips, and G. Simons for many helpful discussions. We are grateful to the donors of the Petroleum Research Fund, sponsored by the American Chemical Society, for partial support of this research.

---

*National Defense Education Act predoctoral trainee.

†Alfred P. Sloan Foundation Fellow.

[1]G. Simons, J. Chem. Phys. 55, 756 (1971).

[2]G. Simons, J. Chem. Phys. 60, 645 (1974).

[3]G. Simons, Chem. Phys. Lett. 12, 404 (1971).

[4]G. Simons, Chem. Phys. Lett. 18, 315 (1973).

[5]G. Simons and A. N. Bloch, Phys. Rev. B 7, 2754 (1973).

[6]A. N. Bloch and G. Simons, J. Amer. Chem. Soc. 94, 8611 (1972).

[7]L. Pauling, *The Nature of the Chemical Bond* (Cornell Univ. Press, Ithaca, N. Y., 1960), 3rd ed.

[8]J. C. Phillips, Phys. Rev. Lett. 20, 550 (1968).

[9]J. C. Phillips, Rev. Mod. Phys. 42, 317 (1970).

[10]See, for example, V. Heine and D. Weaire, in *Solid State Physics*, edited by H. Ehrenreich, F. Seitz, and D. Turnbull (Academic, New York, 1970), Vol. 24, p. 249.

[11]J. C. Barthelot and Ph. Durand, Chem. Phys. Lett. 16, 63 (1972).

[12]This problem is simplified by the appearance of the quantum defect in the orbital rather than the principal quantum number; see Ref. 5.

[13]W. Gordy and W. J. O. Thomas, J. Chem. Phys. 24, 439 (1956).

[14]For a review, see H. O. Pritchard and H. A. Skinner,

Chem. Rev. 55, 745 (1955). In their work with the Mulliken electronegativity scale, Pritchard and Skinner also defined s- and p-orbital contributions to the electronegativity.

[15]H. Jagodzinski, Neues Jahrb. Mineral., Monatsh. 10, 49 (1954).

[16]P. Lawaetz, Phys. Rev. B 5, 4039 (1972).

[17]E. Mooser and W. B. Pearson, Acta Crystallogr. 12, 1015 (1959).

[18]J. A. Van Vechten, Phys. Rev. 187, 1007 (1969).

[19]We are grateful to J. C. Phillips for pointing this out to us.

Tricritical-Point Phase Diagram in $FeCl_2$

R. J. Birgeneau*†
Bell Laboratories, Murray Hill, New Jersey 07974

and

G. Shirane and M. Blume‡
Brookhaven National Laboratory,† Upton, New York 11973

and

W. C. Koehler*†
Oak Ridge National Laboratory,§ Oak Ridge, Tennessee 37830

(Received 15 July 1974)

Detailed measurements of the magnetization and sublattice magnetization of $FeCl_2$ in a magnetic field have been performed by use of polarized- and unpolarized-neutron–diffraction techniques. The phase diagram so determined is found to bear a close resemblance to that of ^{3}He-^{4}He mixtures near the tricritical point although there are a number of important differences which seem to require, at the minimum, an extension of present theories of tricritical phenomena.

In 1935 and 1937 Landau[1] gave a phenomenological theory for thermodynamic systems exhibiting a line of first-order transitions going over continuously into a line of second-order transitions. Three decades later, Graf, Lee, and Reppy[2] showed that just such a situation occurs in ^{3}He-^{4}He mixtures where, at the junction point, the superfluid λ line goes continuously into the phase-separation line. Shortly thereafter, Griffiths[3] considered in more detail the general ^{3}He-^{4}He phase diagram and he showed that the junction point actually occurs at the intersection of three lines of second-order transitions. He thence proposed the name *tricritical point* for this special point on the phase diagram. Griffiths further suggested that tricritical points might occur in a wide variety of physical systems and, in particular, in metamagnets such as $FeCl_2$.[4,5] In this case it is proposed that one has a simple isomorphism between thermodynamic variables with, for example, magnetization $M(H, T) \rightarrow X$, the ^{3}He concentration, and sublattice magnetization $M_s(H, T) \rightarrow |\psi|$, the superfluid order parameter. In this Letter we report a detailed neutron-diffraction study of $FeCl_2$ in a magnetic field. As we shall show, $FeCl_2$ does indeed exhibit tricritical behavior and, furthermore, the phase diagram around the tricritical point bears a close resemblance to that of ^{3}He-^{4}He mixtures. There are, however, a number of quantitative discrepancies with theory which necessitate both an extension of the existing theories together with further experiments.

We consider first the magnetic properties of $FeCl_2$, the experimental technique, and the salient results. We shall then discuss the current theoretical predictions in the context of the results. The crystal structure, magnetic properties, and critical behavior of $FeCl_2$ in zero magnetic field have been extensively discussed by Birgeneau, Yelon, Cohen, and Makovsky.[5] From the vantage point of critical phenomena, $FeCl_2$ may be viewed as being composed of hexagonal sheets of ferromagnetically coupled $S = 1$ Ising spins with successive planes weakly coupled antiferromagnetically. At low temperatures as a function of increasing internal field H_{int} (we shall assume that all fields are applied along the crystalline c axis), $FeCl_2$ undergoes a first-order transition from an antiferromagnetic (A/f) to a